THE ASTROPHYSICAL JOURNAL, 343:678–685, 1989 August 15

THE ORIGIN OF CORONAL LINES IN SEYFERT GALAXIES

K. T. KORISTA AND G. J. FERLAND
Ohio State University
Received 1988 December 9; accepted 1989 January 24

ABSTRACT

In this paper we examine the possibility that the coronal line region in Seyfert galaxies may be the result of an interstellar medium (ISM) exposed to, and subsequently photoionized by, a "bare" Seyfert nucleus. We show that a "generic" AGN continuum illuminating the warm-phase ($N_e \sim 1$ cm^{-3}) of the ISM of a spiral galaxy can produce the observed emission. In this picture the same UV-radiation cone that is responsible for the high-excitation extended narrow-line emission clouds observed out to 1–2 kpc or farther from the nuclei of some Seyfert galaxies also produces the coronal lines. Soft X-rays originating in the nucleus are Compton-scattered off the ISM, thus producing extended soft X-ray emission, as observed in NGC 4151. The results of our calculations show a basic insensitivity to the ISM density, which explains why similar coronal line spectra are found in many Seyfert galaxies of varying physical environments.

Subject headings: galaxies: interstellar matter — galaxies: Seyfert — radiation mechanisms

I. INTRODUCTION

The broad permitted emission lines observed in active galactic nuclei (AGN) originate in gas having densities greater than 10^9 cm^{-3}, from a region less than a parsec from the central continuum source (see, for example, Davidson and Netzer 1979). The narrow lines are emitted in regions of densities 10^3–10^6 cm^{-3} lying 10–10^3 parsecs out. Photoionization by the central continuum source is probably the dominant ionization mechanism in both regions (Davidson and Netzer 1979). However, the very high excitation forbidden lines of [Fe VII] λ6087, [Fe X] λ6375, [Fe XI] λ7892, and [Fe XIV] λ5303 (the so-called iron "coronal" lines) do not seem to fit into either of the above niches. These lines may have widths intermediate between the lower excitation narrow lines and the broad lines, and are usually blueshifted relative to the lower excitation narrow lines (DeRobertis and Osterbrock 1984, 1986; Grandi 1978; Osterbrock 1981; Osterbrock and Pogge 1985; Penston *et al.* 1984). Their critical densities ($\sim 10^7$ cm^{-3} for [Fe VII] to $\sim 10^{10}$ cm^{-3} for [Fe X]) are also intermediate (DeRobertis and Osterbrock 1986); [Fe X] λ6375 could originate in regions as dense as 6×10^{11} cm^{-3} (Penston *et al.* 1984), although there is no observational lower limit to the density. The above observations, plus the possible relationship between a narrow forbidden line's FWHM and its ionization potential or critical density (DeRobertis and Osterbrock 1984, 1986; Osterbrock 1981; Filippenko and Halpern 1984), suggested to earlier investigators that the "coronal" line region (CLR) lies within a transition zone between the broad-line region (BLR) and the narrow-line region (NLR), a zone of intermediate densities and velocities. All previous "scenarios" for the formation of the coronal lines (there have been few self-consistent calculations) have assumed this.

Previous investigations have postulated that the CLR is either a hot (10^6 K), collisionally ionized gas (Oke and Sargent 1968; Nussbaumer and Osterbrock 1970) or a cooler gas (10^4 K) photoionized by the central continuum source (Osterbrock 1969; Nussbaumer and Osterbrock 1970; Grandi 1978). Photoionization in combination with shocks has also been proposed (Viegas-Aldrovandi and Contini 1989). Here we investigate a very simple origin of the coronal lines, in the spirit of the second hypothesis. The AGN phenomenon is known to occur within a galactic environment (see Begelman 1985; Chang, Schiano, and Wolfe 1987). We show that a typical galactic interstellar medium ($N_e \sim 1$ cm^{-3}) photoionized by a "bare" Seyfert nucleus is all that is required to produce the coronal lines.

In § II, we discuss coronal line formation. The results of our model along with comparisons with observations are presented in § III. Finally, a summary is provided in § IV.

II. LINE FORMATION

a) *Photoionization Code and Atomic Data*

Ionization and thermal equilibrium calculations were performed with the photoionization code "Cloudy" most recently described by Ferland and Rees (1988) and Ferland and Persson (1989). Here we discuss some details relevant to coronal line formation.

Iron photoionization cross sections, recombination coefficients, and collisional ionization rate coefficients are taken from Reilman and Manson (1979), Woods, Shull, and Sarazin (1981), and Arnaud and Rothenflug (1985), respectively. The collision strengths are from Mason (1975) (Fe X, Fe XI, and Fe XIV) and Nussbaumer and Storey (1982) (Fe VII); the transition probabilities for the iron coronal lines are from Smith and Wiese (1973), Mendoza and Zeippen (1983) and Fuhr *et al.* (1981). Charge transfer rate coefficients for reactions between iron and hydrogen come from Neufeld (1984), and K shell fluorescent yields from Krolik and Kallman (1987). We know of no calculation of rate coefficients for iron dielectronic recombination through low-lying autoionizing states. This makes the ionization balance uncertain by roughly a factor of 2.

b) *Radiative Pumping and Collisional Excitation*

Many iron lines can be both collisionally excited and radiatively pumped by electron dipole transitions in the extreme ultraviolet ($\sim$300 Å). For temperatures typical of the solar corona ($T \sim 10^6$ K) collisional excitation of these lines occurs mainly via excitation to higher lying levels, followed by radiative decay to the upper level of the observed transition, and

effective collision strengths which incorporate these decays are often defined (see, for example, Mason 1975). For the present application temperatures are too low for this to occur, and tests show that collisional excitation directly to the upper level of the observed transition is the major contributor to the collisional rate. Energy level diagrams for the ions we model are shown in Figure 1; the ultraviolet pumping mechanisms we include are also shown along with the coronal line transitions themselves. For [Fe X] λ6375 ($^2P^o_{3/2}$–$^2P^o_{1/2}$) we include collisional excitation to $^2P^o_{1/2}$ from the ground state and electric dipole continuum pumping to $^2S_{1/2}$ from the ground state (345.75 Å) and subsequent decay to $^2P^o_{1/2}$ (365.57 Å), populating the upper level of the 6375 Å line. For [Fe XIV] λ5303 ($^2P^o_{1/2}$–$^2P^o_{3/2}$) we include collisional excitation to $^2P^o_{3/2}$ from the ground state and electric dipole continuum pumping to $^2D_{3/2}$ from the ground state (334.15 Å) and subsequent decay to $^2P^o_{3/2}$ (356.60 Å). Collisional excitation to $^3P_1$, $^3P_0$ and electric dipole continuum pumping to $^3P^o_1$ (341.115 Å) and $^3P_2$ (352.680 Å) from the ground state of Fe XI are included for the 7892 Å line ($^3P_2$–$^3P_1$). Here we neglect collisional deexcitation of $^3P^o$, a good assumption under the physical conditions considered here. The [Fe VII] λ6087 line is a $^3F_3$–$^1D_2$ transition. Continuum pumping does not contribute to this line due to forbidden spin changes that must occur, thus no fluorescence. Collisional excitation to the upper level is considered

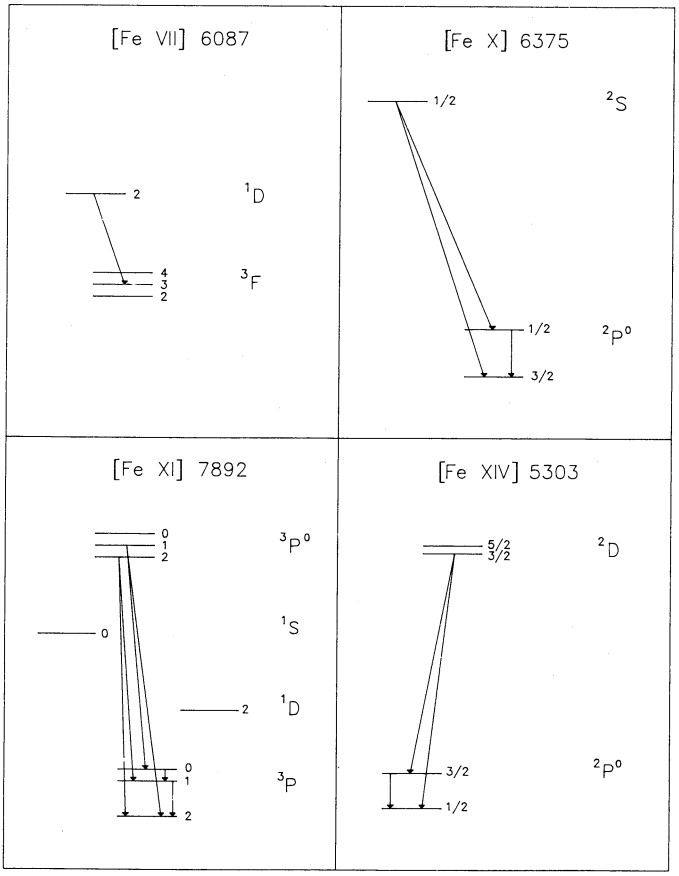

FIG. 1.—Illustrated here in these partial Grotrian diagrams are the continuum pumping transitions and the four iron coronal line emission transitions considered in this model. The [Fe VII] λ6087 transition is (*lower–upper*) $^3F_3$–$^1D_2$, that of [Fe X] λ6375 is $^2P^o_{3/2}$–$^2P^o_{1/2}$, that of [Fe XI] λ7892 is $^3P_2$–$^3P_1$, and that of [Fe XIV] λ5303 is $^2P^o_{1/2}$–$^2P^o_{3/2}$.

(Nussbaumer and Osterbrock 1970; Nussbaumer and Storey 1982; Sugar and Corliss 1985).

The ultraviolet pump transitions become optically thick (with optical depths of many); we assume the formalism of Ferland and Rees (1988) and a *micro*turbulent velocity field of 350 km s^{-1}, which has the effect of increasing the bandwidth and reducing the optical depth within the pump transitions (τ becomes 0.719 from 62.6 for the [Fe X] pump transition, 0.522 from 37.9 for [Fe XI], and 0.260 from 11.0 for [Fe XIV] for an interstellar medium [ISM] density of 1.0 cm^{-3}). The value was chosen to reflect the observed line width of the [Fe X] λ6375 line in NGC 4151 (Penston *et al.* 1984). Much of the observed width is actually due to bulk motions (*macro*turbulence), but the effect of either velocity field on the pumping rate is nearly the same. These pumping transitions are important, as they often produced more than 50% of the line intensity. It is important to remember that the actual continuum shape near ~300 Å (the region most efficient in pumping the iron lines) is largely unexplored—this is an unavoidable uncertainty in addition to the uncertainty in the atomic data (many of the transition probabilities for the iron ions are uncertain by a factor of 2, according to Fuhr *et al.* (1981); the model does not include iron dielectronic recombination through low-lying autoionizing states, since these recombination coefficients have not been computed). As a result we anticipate at least a factor of 2 uncertainty in the predicted line fluxes and shall consider any better agreement between observation and prediction to be a success.

c) *The Model Continuum*

We use the mean AGN continuum deduced by Mathews and Ferland (1987), but with a break in the infrared continuum at 10 μm; the wavelength of this submillimeter break has no effect on the following calculations. The continuum intensity is scaled to NGC 4151's flux at 912 Å (we assume $\nu L_\nu(912\text{ Å}) = 10^{43}$ erg s^{-1} from Ferland and Mushotzky (1982) for an H_0 of 55 km s^{-1} Mpc^{-1} and a distance to NGC 4151 of 20 Mpc) in order that we can make semiquantitative comparisons of line luminosities, line ratios, and other physical phenomena for this object. However, we choose a *mean* AGN continuum so that our model can be as general as possible to explain a common phenomenon in Seyfert galaxies and do not intend to model the CLR in any one particular AGN. In Figure 2 we show a portion of the incident continuum (*solid line*) (the resulting transmitted spectrum [*dots*] will be discussed later).

d) *Model Geometry*

Although the distribution of the ISM is not as well known near the centers of spiral galaxies (or Seyferts) as in the outer regions, we assume a flattened geometry like that of the latter region. The disk of our model has an inner radius of 10 pc (the conventional inner radius of the NLR) and an outer radius of 2 kpc, and a semithickness of 100 pc (about one gas and dust scale height in the spiral arm region of the Galaxy [Mihalas and Binney 1981]). The choice of outer radius was set by the requirement that the CLR extend to at least the observed radii of some of the Seyfert nucleus-excited *extended* narrow-line regions (ENLR) observed (Heckman and Balick 1983; Schulz 1988; Unger *et al.* 1987, 1988; and others). We also investigated a spherical gas distribution; the differences were not large compared to other uncertainties, such as the intensity of the ~300 Å continuum.

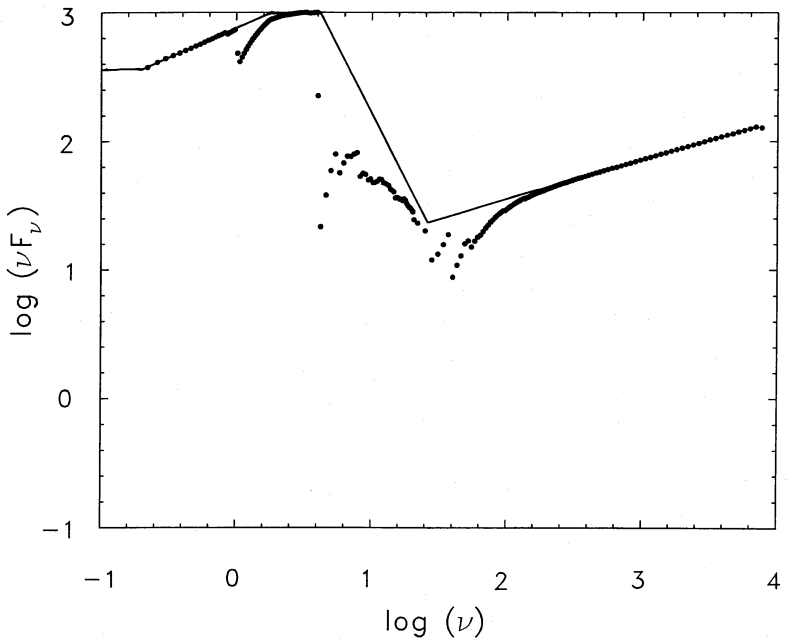

FIG. 2.—Part of the incident continuum (*solid line*) and the resultant transmitted spectrum (*dots*) for a hydrogen density of 0.5 cm^{-3}, plotted in log (νF_ν) vs. log ν(rydberg) units. Density is measured in cm^{-3} and flux density has units of ergs s^{-1} cm^{-2} ryd^{-1}. Note the Lyman limit absorption, the He II edge, and the various *K* shell absorptions.

e) Abundances and Dust

We assume solar abundances and a constant, uniform hydrogen density, with a filling factor of unity. Abundances are quite uncertain; however, tests show that changing the abundance of oxygen (several ionization stages of oxygen are major coolants in our model) by a factor of 2 from solar affects the iron coronal lines very little.

Several lines of evidence suggest that dust is underabundant in the diffuse gas. The X-ray column densities estimated by Mushotzky, Holt, and Serlemetsos (1978) in NGC 4151 ($\geq 3 \times 10^{22}$ atoms per cm^{-2}) would imply a reddening due to dust of $A_v \geq 13$ mag given the Galactic dust-to-gas ratios, but the observed optical reddening is $A_v \leq 0.2$ mag (Wu and Weedman 1978). This discrepancy implies a dust-to-gas ratio of $\leq 1/200$ that of "normal," for the gas on the line of sight to the X-ray emitting region. The presence of normally refractory elements, such as iron, in the gas phase also suggests that depletion is not extreme. Sufficient iron must be present in its gas phase and not condensed onto grains (as is observed in the general ISM; Morton 1978) for the iron coronal lines to be present. It is easy to show, however, that our model continuum does not destroy dust grains by sublimation in the coronal line emitting regions on any reasonable time scales (Draine and Salpeter 1979). It is possible that other dust destruction mechanisms are at work (see also Begelman 1985; Chang, Schiano, and Wolfe 1987). Accordingly, we include the effects of dust, as discussed by Martin and Ferland (1980), assuming a dust-to-gas ratio 0.005 of Galactic, i.e., $\sigma_{scat}(V)/N_H = 2.5 \times 10^{-24}$ cm^5. This dust abundance is low enough to have little effect on the following calculations.

III. THE MODEL RESULTS

a) Coronal Line Intensities and Ratios

Given the assumptions outlined above, the only remaining free parameter is the hydrogen density, N_H (cm^{-3}), which we vary. The predicted line luminosities and ratios as a function of the hydrogen density are shown in Figure 4 and Table 1. These predictions are to be compared with Table 2, which summarizes observations of NGC 4151. In Table 2 we assume an [O III] λ5007 flux of $(1.19 \pm 0.06) \times 10^{-11}$ ergs cm^{-2} s^{-1} (Antonucci and Cohen 1983; this was needed to normalize those line intensities which are given relative to [O III] λ5007 in some studies). Table 3 lists the predicted relative strengths of other prominent lines for a density $N_H = 1.0$ cm^{-3}.

The behavior of the line ratios shown in Figure 4 are the result of the interplay between changes in the mean ionization of the gas and the radial distribution of the ions. For a given ionization rate Γ (s^{-1}) and recombination coefficient α (cm^3 s^{-1}) (see Osterbrock 1988), the ionization balance between adjacent stages of ionization is simply

$$N^{i+1}/N^i \sim \Gamma/(N_H \alpha) \sim {N_H}^{-1} ,$$

TABLE 1

MODEL CORONAL LINE LUMINOSITIES AND LINE RATIOS

log [N_H(cm^{-3})]	log (Fe VII)	log (Fe X)	log (Fe XI)	log (Fe VII / Fe X)	log (Fe XI / Fe X)	log (Fe XIV / Fe X)	log (Fe VII / Fe XI)
0.0	38.906	38.888	38.634	0.018	−0.254	−1.023	0.272
0.5	39.213	39.327	39.091	−0.114	−0.236	−1.009	0.122
1.0	39.513	39.723	39.487	−0.210	−0.236	−1.100	0.026

TABLE 2

IRON CORONAL LINE OBSERVATIONS OF NGC 4151

Line or Line Ratio	log (Line Ratio and Luminosity)	Reference
[Fe VII] 6087	39.92	Penston *et al.* 1984; Grandi 1978
	39.92	Boksenberg *et al.* 1975
	39.79	Osterbrock and Koski 1976
	39.80	Peterson *et al.* 1982
	39.86	OSU-unpublished
Mean	39.86 ± 0.06	
[Fe X] 6375	39.23	Penston *et al.* 1984
	39.53	Osterbrock and Koski 1976
	39.80	OSU-unpublished
Mean	39.52 ± 0.29	
[Fe XI] 7892	39.53	Penston *et al.* 1984; Grandi 1978
[Fe VII]/[Fe XI]	0.39	Penston *et al.* 1984; Grandi 1978
	0.26	
Mean	0.33	
[Fe VII]/[Fe X]	0.69	Penston *et al.* 1984
	0.27	Osterbrock and Koski 1976
	0.60	Pelat, Alloin, and Bica 1987
	0.53	Oke and Sargent 1968
	0.27	Souffrin 1968
	0.06	OSU-unpublished
Mean	0.40 ± 0.24	
[Fe XI]/[Fe X]	0.30	Penston *et al.* 1984
	0.35	Pelat *et al.* and Grandi 1978
Mean	0.33	
[Fe XIV]/[Fe X]	−0.12	Pelat *et al.*

TABLE 3

MODEL RELATIVE CORONAL LINE REGION LUMINOSITIES FOR AN INTERSTELLAR MEDIUM DENSITY $N_H = 1.0$ cm^{-3}

Ion (1)	λ(Å or μm) (2)	$L/L(H\beta)$ (3)
O VI	1035	3.605
Lyα	1216	23.018
O V	1218	1.392
N V	1240	0.670
C IV	1549	1.991
He II	1640	2.386
C III]	1909	0.145
[Fe XII]	2170	0.035
Mg VII	2629	0.192
Ne V	3426	0.972
Hδ	4102	0.297
Hγ	4340	0.505
He II	4686	0.314
Hβ	4861	1.000
[O III]	5007	7.271
[Fe XIV]	5303	0.008
[Fe VII]	6087	0.087
[Fe X]	6375	0.083
Hα	6563	2.699
[Fe XI]	7892	0.046
[Si VI]	1.9 μm	0.172
[Mg V]	5.6 μm	0.784
[Ne VI]	7.6 μm	0.332
[S IV]	10.5 μm	1.707
[Ne V]	14.3 μm	0.200
[Ne V]	24.2 μm	0.371
[O IV]	26.0 μm	5.160
[Ne VII]	77.4 μm	0.114
[O III]	88.0 μm	6.114

log L (Hβ) = 39.967

so lower densities favor higher ionization. In Figure 4 the rapid decrease in intensity of lines from higher stages of ionization at higher densities is caused by the relatively low abundances of these ions.

The Strömgren radius R_S is also inversely proportional to radius. For an extended geometry,

$$R_S \sim Q(\mathrm{H})^{1/3} N_H^{-2/3} ,$$

where Q(H) is the number of hydrogen ionizing photons (Osterbrock 1988). As a result, the radial scale of the ionization structure shown in Figure 5 (for a density of $N_H = 1.0$ cm^{-3}) also scales inversely with density. In the calculations the outer radius was held fixed, and as a result for densities much below ~0.5 cm^{-3} the [Fe VII] line is depressed because the Fe^{6+} zone occurs beyond the outer radius.

The relative line intensities change little between densities of ~0.5 cm^{-3} and 10^3 cm^{-3}. Here, densities are low enough for all of the relevant stages of ionization to be populated, but yet high enough for all ionization stages to be within the fixed inner and outer radii. This insensitivity to density (the one remaining parameter) is a major success for the present model. Figures 2 and 3 show both the incident (*solid line*) and transmitted (*dotted line*) continuum for two typical densities (N_H = 0.5, 1.0 cm^{-3}). Objects which we view directly through the disk of the ISM will show moderate-to-extreme soft X-ray absorption. This presents a test of the model.

Given the uncertainties in some of the atomic physics and the difficulty in measuring these weak (usually a few percent of [O III] λ5007) and sometimes blended lines, it is not surprising that there are some differences between Tables 1 and 2. One must note, however, that most of the predicted line lumin-

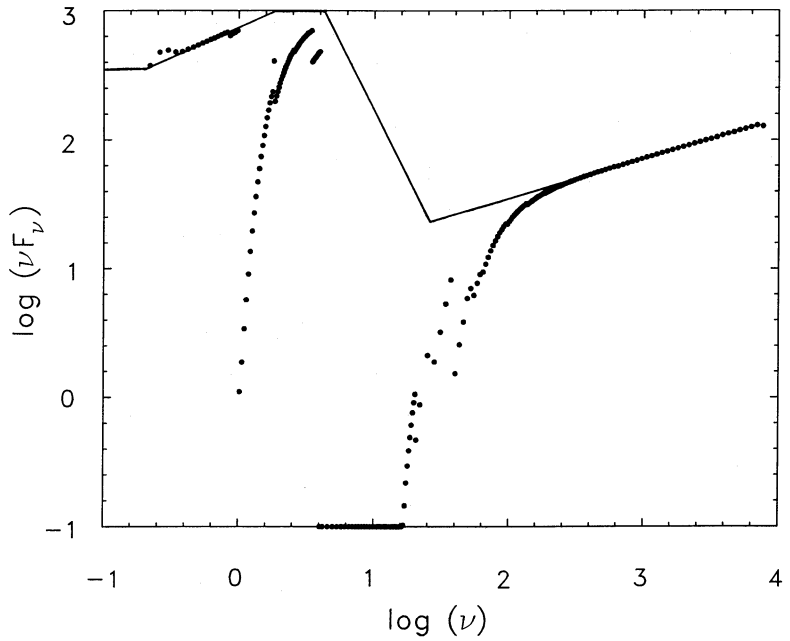

FIG. 3.—Same as Fig. 2 except for a hydrogen density of 1.0 cm^{-3}. The line of dots near 10 rydbergs are off scale and lie much lower. Note the prominent Lyman limit, He I, and He II edges. Note also some reemission in the blue/near-UV due to balmer continuum emission.

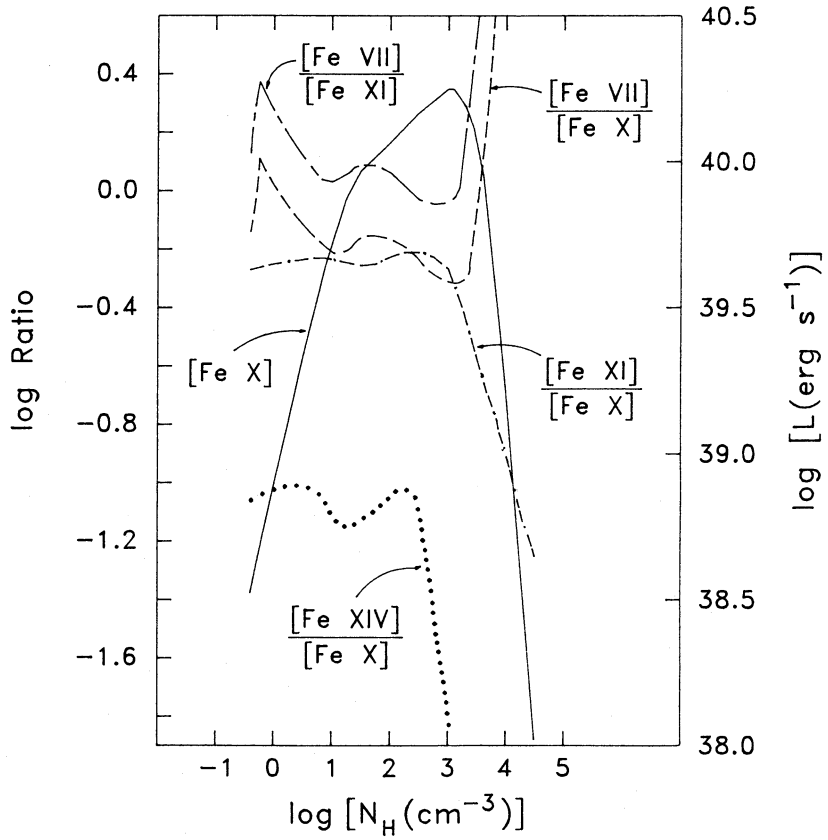

FIG. 4.—Model results of the log of the luminosity (ergs s^{-1}) of the [Fe X] λ6375 line, and the log of the luminosity ratios [Fe VII] λ6087, [Fe XI] λ7892, and [Fe XIV] λ5303 to [Fe X] λ6375 and that of [Fe VII] λ6087 to [Fe XI] λ7892 as a function of the log of the hydrogen density in cm^{-3}.

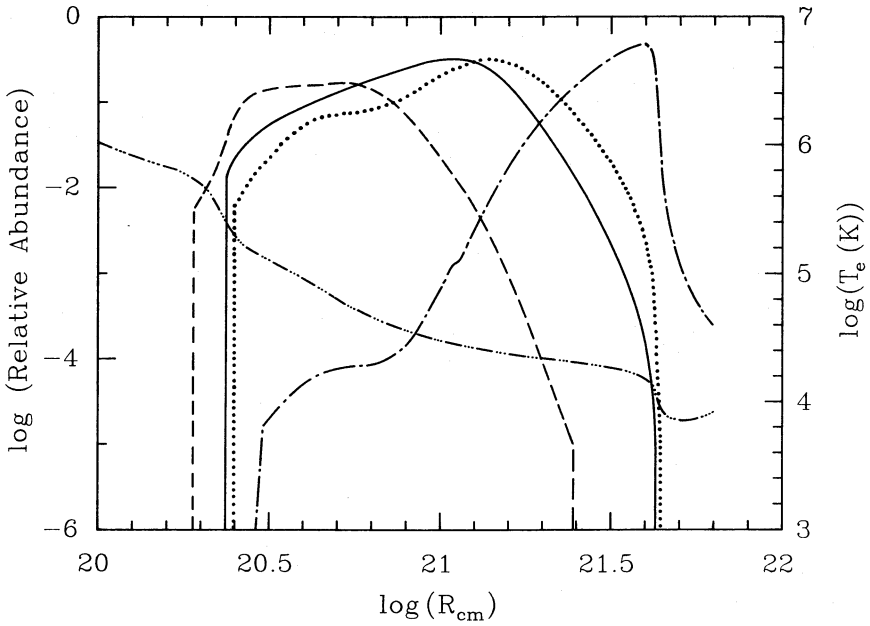

FIG. 5.—The relative abundance of the four iron ions and the electron temperature as a function of distance from the central source on a log-log plot for a hydrogen density of 1.0 cm^{-3}. The relative abundance of Fe^{13+} is represented by the dashed line, that of Fe^{10+} by the solid line, that of Fe^{9+} by the dotted line, and that of Fe^{6+} by the dash-dot-dash line. The electron temperature is indicated by the dash-triple dot-dash line.

osities and ratios of [Fe VII], [Fe X], and [Fe XI] all lie within a factor of 2 or 3 of the observed values. The small predicted [Fe XIV]/[Fe X] ratio is consistent with the fact that [Fe XIV] is rarely observed (see Osterbrock 1981; Pelat, Alloin, and Bica 1987; Ward and Morris 1984 for possible observations of this line).

We emphasize again that we have not attempted to present a finely tuned model. One must keep in mind that our *mean* AGN model continuum was merely scaled to match the continuum intensity of NGC 4151 at 912 Å. The strength and shape of the continuum in the ~300 Å and 100–400 eV regions is certainly important; however, we find that choosing different reasonable continua shapes (see, for example, Elvis 1987) does not produce qualitative differences. This simple model may be all that is necessary to produce the observed coronal lines in Seyfert galaxies.

b) The Size and Environment of the Coronal Line Region

The model predicts that the CLR should be quite extended and spatially resolved in some cases. The distance (R_{max}) from the central continuum source at which the coronal line emissivity is maximum, typical electron temperatures ($T_e[R_{max}]$), and the effective emitting range (ΔR) (where the fractional ionization for ion is greater than approximately 10%) for different densities are shown in Table 4. Figure 5 shows, for one density, the electron temperature and ionization structures. The temperatures in the emitting regions are typical of nebular temperatures, and the emission regions span much of the NLR and perhaps beyond. The former result has been found to be true for at least [Fe VII] (Boksenberg *et al.* 1975; Osterbrock 1981; Fosbury and Sansom 1983), while the latter result should be observationally testable (spatially resolvable) for some of the more nearby Seyfert galaxies with strong coronal lines (NGC 4151, NGC 1068). Also note from Table 4 the size of the emitting regions—tens to hundreds of parsecs—and that there is some overlap in the emitting regions. Coronal line variability is then another observational test of the model; the coronal lines should not vary over time scales of a month to a year (see Veilleux 1988*a*), due to the extended nature of the emitting region. For reasons discussed above, the higher ionization stages tend to occur at smaller radii and over smaller ranges. As one might expect, [Fe VII] and [Fe X] have the largest R_{max} and would therefore be easiest to test the extendedness of the CLR. R_{max} is independent of the geometry we use and is mainly dependent upon the number of ionizing/exciting photons and electron density.

Several other lines are predicted to be strong; see Table 3. The [Fe XII] λ2170 line is predicted to be typically ~40% or so of [Fe X] λ6375, although confirmation of this line and its strength will probably have to await the Hubble Space Telescope (HST). The model predicts that the CLR produces significant [Ne V] λ3426 emission, typically ~12 times the strength of the [Fe X] line. Extended [Ne V] emission is sometimes seen (Ward 1988). Many of the other lines given in Table 3 are also produced in the NLR, so it would be difficult to test those predictions observationally.

c) A Possible Coronal Line Region, Extended Narrow-line Region, and Radio Jet Connection

The orientation of the radio jet relative to the galactic disk may be important in determining the strength of the coronal line region. In two galaxies where an ENLR has been observed and the radio jet lines *within* the galactic disk in the direction of the ENLR (NGC 4151, NGC 1068) (Wilson and Ulvestad 1982; Heckman and Balick 1983; Unger *et al.* 1987, 1988; Schulz 1988), strong coronal lines are observed (Penston *et al.* 1984). In NGC 4388, in which extended (noncoronal line) emission due to the Seyfert nucleus is observed above and below the galactic disk, the radio jet lies along the direction of the ENLR but *perpendicular* to the galactic disk, and at least [Fe X] λ6375 is very weak or absent (Corbin, Baldwin, and Wilson 1988; Filippenko and Sargent 1985; Shields 1988); the

TABLE 4

TYPICAL ELECTRON TEMPERATURES, RADII, AND EFFECTIVE EMITTING RANGES AT MAXIMUM EMISSIVITY

Ion	log [N_H(cm^{-3})]	$T_e(R_{max})$	R_{max}(pc)	ΔR(pc)
Fe VII	0.0	16,000 K	1200	745–1400
	0.5		610	350–660
	1.0		290	210–300
Fe X	0.0	26,000 K	420	200–750
	0.5		245	110–415
	1.0		130	75–200
Fe XI	0.0	28,000 K	350	130–520
	0.5		200	85–290
	1.0		110	45–160
Fe XIV	0.0	70,000 K	145	80–200
	0.5		85	45–140
	1.0		45	25–70

other coronal lines have not been well studied. In all three cases the ENLR lies in the direction of the radio jet which may represent the escape route of the nuclear radiation exciting the CLR and ENLR, but the coronal lines appear to be strong only when the radio jet lines in the galactic plane. It is possible that there is insufficient ISM being hit by the Seyfert nucleus, if it is preferentially "beamed" perpendicular to the galactic disk, to produce strong coronal lines, in objects where the radio jet does not lie within the disk. This is consistent with our model, and may be evidence that the radio jet or inner radio structure, an anisotropic nuclear radiation field, the CLR, and the ENLR are all in some way interconnected.

In recent years large amounts of observational evidence has been amassed supporting the picture that the ENLR in Seyfert galaxies is excited by a bare anisotropic Seyfert radiation field and lies along the direction of a nuclear radio jet (see, for example, Heckman and Balick 1983; Unger *et al.* 1987, 1988; Corbin, Baldwin, and Wilson 1988; Schulz 1988; and references therein). The coronal line region should also see a bare Seyfert nucleus. Thus another observational test is the predicted relationship between the CLR and the ENLR; i.e., does the CLR lie along the same direction as the ENLR, implying that the CLR has a clear view of the Seyfert nucleus? If the ENLR and the CLR are indeed seeing the same bare Seyfert nucleus, then in principle an upper limit to the warm-phase ISM density in the direction of the ENLR and thus that in the CLR can be established.

d) Soft X-Ray Extension

A final result of our model is that the predicted Compton scattering optical depths are sufficient to explain the extended soft X-ray emission observed by Elvis, Briel, and Henry (1983) in NGC 4151 as simply nuclear X-rays scattering off the coronal line gas. The optical depth to electron scattering (radially) through the disk is $\tau_e \approx 0.005(1.0\ \mathrm{cm}^3\ N_H)$. This relation holds while the gas is fully ionized; an ionization front occurs when $N_H \approx 4\ \mathrm{cm}^{-3}$; then $\tau_e \approx 0.020$. We expect this medium to scatter a fraction $(1 - e^{-\tau}) \sim \tau \sim$ a few percent of the incident radiation field. This is sufficient to explain the observed soft X-ray extension in NGC 4151 as simply scattered *unextinguished* nuclear continuum. The intrinsic soft X-ray continuum, extrapolated from the hard X-ray observations of Holt *et al.* (1980) assuming no extinction, amounts to ~ 1.7 counts s^{-1} keV^{-1} at 0.5 keV. The CLR will scatter $\sim 1\%$ of this (depending on the density), and this is sufficient to account for the less than or equal to 30% *extension* contribution to the *total* soft excess component flux observed in NGC 4151 (Elvis, Briel, and Henry 1983; Perola *et al.* 1986; Pounds *et al.* 1986). One might then expect that other Seyfert galaxies exhibiting ENLRs and CLRs that lie in the disk of the galaxy to have extended soft X-ray regions as well; we just have not been able to resolve them.

e) Kinematics and Line Width

The model does not attempt to explain the structure or kinematics of the coronal line emitting region; there are some indications that at least the [Fe VII] lines arise from multiple components (and plausibly multiple mechanisms) in some Seyfert galaxies. These lines show large blueward asymmetries in at least one Seyfert galaxy (Mrk 359) in the sample studied by Veilleux (1988*b*). Our calculations, and others, suggest that [Fe VII] also has a contribution from the NLR, so several regions are expected to contribute to the net profile of this line.

As a further complication, it can be shown that the nuclear continuum can radiatively accelerate the low-density gas, in the presence of *some* dust, to large velocities ($\sim 10^3$ km s^{-1}) over distances of order the CLR. The major uncertainty in this is the actual amount of dust present in the ISM. If an appreciable fraction of the carbon is in graphite in the CLR, then effective radiative acceleration is inevitable, so that the coronal line widths will not reflect the rotation velocity of the galaxy. Further dynamical considerations along these lines are presented by Chang *et al.*

IV. CONCLUSIONS

This paper presents calculations examining the effects of a bare Seyfert galaxy continuum on the surrounding interstellar medium. These calculations show that high-ionization lines are produced, with relative intensities quite similar to those observed. The line strengths and ratios show a basic insensitivity to density. In this picture the observed soft X-ray extension is the result of electron scattering off the ISM. This model is open to several observational tests. These are the following.

1. *Spatial Extent.*—We predict the coronal line region to lie at or beyond the narrow-line region, in a direction with an unobscured view of the nucleus. Thus it should be resolvable, at least for nearby objects. The resolved CLR should lie in the same direction as the extended NLR emission and radio emis-

sion. The CLR could provide a mechanism to map the anisotropic radiation field of the nucleus.

2. *Variability.*—The high-ionization lines should not be variable. Variability over time scales of a month to a year would require that the bulk of the gas be closer to the nucleus than we predict (see Veilleux [1988*a*] for a recent variability study). However, we do predict that the CLR should lie over an angular extent of several to 10 seconds of arc for some of the nearby Seyfert galaxies. Typical entrance apertures are often of order this size, so that small centering errors can affect the line strengths. Very large apertures and careful centering are needed to measure these line strengths reliably.

3. *Kinematics.*—The line profile, produced by the gas we model, should characterize low-density gas at large radius. We do not address kinematics or the observed coronal line profiles in this paper. However, it has been shown (Chang, Shiano, and Wolfe 1987) that radiative acceleration of the host galaxy ISM due to the AGN continuum is significant, and might, therefore, contribute to the dynamics of the coronal line emitting region. Given the complexity of the AGN phenomenon, it would be surprising if other gas, perhaps a smaller radii, did not also exist. High spectral resolution, high signal-to-noise, spatially resolved observations will provide a decisive test of this model.

We gratefully acknowledge informative discussions and correspondences with J. Baldwin, M. Corbin, M. Elvis, M. Penston, J. Shields, S. Veilleux, J. Villumsen, and M. Ward. We also thank M. Penston, J. Shields, and S. Veilleux for sending us some of their data, and P. Stoycheff for the figures and tables. G. J. F. acknowledges the financial support of the NSF (AST 87-19607). K. T. K. thanks B. M. Peterson for his support and guidance, and acknowledges two years of support as the Perkins Fellow. This work is part of K. T. K.'s doctoral dissertation to be submitted in partial fulfillment of degree requirements at the Ohio State University.

REFERENCES

Antonucci, R., and Cohen, R. 1983, *Ap. J.*, **271**, 564.
Arnaud, M., and Rothenflug, R. 1985, *Astr. Ap. Suppl.*, **60**, 425.
Begelman, M. C. 1985, *Ap. J.*, **297**, 492.
Boksenberg, A., *et al.* 1975, *M.N.R.A.S.*, **173**, 381.
Chang, C. A., Schiano, A. V. R., and Wolfe, A. M. 1987, *Ap. J.*, **322**, 180.
Corbin, M., Baldwin, J., and Wilson, A. 1988, *Ap. J.*, **334**, 584.
Davidson, K., and Netzer, H. 1979, *Rev. Mod. Phys.*, **51**, 715.
DeRobertis, M. M., and Osterbrock, D. E. 1984, *Ap. J.*, **286**, 171.
———. 1986, *Ap. J.*, **301**, 727.
Draine, B. T., and Salpeter, E. E. 1979, *Ap. J.*, **231**, 438.
Elvis, M. 1987, in *Rutherford Appleton Laboratory Workshop on Astronomy and Astrophysics: Emission Lines in Active Galactic Nuclei*, ed. P. M. Gondhalekar, p. 20.
Elvis, M., Briel, U. G., and Henry, J. P. 1983, *Ap. J.*, **268**, 105.
Ferland, G. J., and Mushotzky, R. F. 1982, *Ap. J.*, **262**, 564.
Ferland, G. J., and Persson, E. 1989, *Ap. J.*, submitted.
Ferland, G. J., and Rees, M. J. 1988, *Ap. J.*, **332**, 141.
Filippenko, A. V., and Halpern, J. P. 1984, *Ap. J.*, **285**, 458.
Filippenko, A. V., and Sargent, W. 1985, *Ap. J. Suppl.*, **57**, 503.
Fosbury, R., and Sansom, A. 1983, *M.N.R.A.S.*, **204**, 1231.
Fuhr, J. R., *et al.* 1981, *J. Phys. Chem. Ref. Data*, **10**, 397.
Grandi, S. A. 1978, *Ap. J.*, **221**, 501.
Heckman, T. M., and Balick, B. 1983, *Ap. J.*, **268**, 102.
Holt, S. S., *et al.* 1980, *Ap. J.* (*Letters*), **241**, L13.
Krolik, J., and Kallman, T. 1987, *Ap. J.* (*Letters*), **320**, L5.
Mason, H. 1975, *M.N.R.A.S.*, **170**, 651.
Martin, P. G., and Ferland, G. J. 1980, *Ap. J.* (*Letters*), **235**, L125.
Mathews, W. G., and Ferland, G. J. 1987, *Ap. J.*, **323**, 456.
Mendoza, C., and Zeippen, C. J. 1983, *M.N.R.A.S.*, **202**, 981.
Mihalas, D., and Binney, J. 1981, *Galactic Astronomy* (San Francisco: Freeman).
Morton, D. 1978, *Ap. J.*, **222**, 863.
Mushotzky, R. F., Holt, S. S., and Serlemetsos, P. J. 1978, *Ap. J.* (*Letters*), **225**, L115.
Neufeld, D. A. 1984, Harvard University Research Exam.
Nussbaumer, H., and Osterbrock, D. E. 1970, *Ap. J.*, **161**, 811.
Nussbaumer, H., and Storey, P. J. 1982, *Astr. Ap.*, **113**, 21.
Oke, S., and Sargent, W. 1968, *Ap. J.*, **151**, 807.
Osterbrock, D. E. 1969, *Ap. Letters*, **4**, 57.
———. 1981, *Ap. J.*, **246**, 696.
Osterbrock, D. E., and Koski, A. T. 1976, *M.N.R.A.S.*, **176**, 61P.
Osterbrock, D. E., and Pogge, R. 1985, *Ap. J.*, **297**, 166.
Osterbrock, D. E. 1988, *Astrophysics of Gaseous Nebulae and Active Galactic Nuclei* (Mill Valley: University Science Press).
Pelat, D., Alloin, D., and Bica, E. 1987, *Astr. Ap.*, **182**, 9.
Penston, M. V., *et al.* 1984, *M.N.R.A.S.*, **208**, 347.
Perola, G. C., *et al.* 1986, *Ap. J.*, **306**, 508.
Peterson, B. M., Foltz, C. B., Byard, P. L., and Wagner, R. M. 1982, *Ap. J. Suppl.*, **49**, 469.
Pounds, K. A., *et al.* 1986, *M.N.R.A.S.*, **218**, 685.
Reilman, R. F., and Mason, S. T. 1979, *Ap. J. Suppl.*, **40**, 815.
Schulz, H. 1988, *Astr. Ap.*, **203**, 233.
Shields, J. 1988, private communication.
Smith, M. W., and Wiese, W. L. 1973, *J. Phys. Chem. Ref. Data*, **2**, 85.
Souffrin, S. 1968, *Ann. d'Ap.*, **31**, 569.
Sugar, J., and Corliss, C. 1985, *J. Phys. Chem. Ref. Data*, **14**, Suppl. 2.
Unger, S. W., *et al.* 1987, *M.N.R.A.S.*, **228**, 671.
Unger, S. W., *et al.* 1988, paper presented at IAU Symposium 134, *Active Galactic Nuclei*, Santa Cruz, CA, in press.
Veilleux, S. 1988*a*, *A.J.*, **95**, 1695.
———. 1988*b*, private communication; and paper presented at IAU Symposium 134, *Active Galactic Nuclei*, Santa Cruz, CA, in press.
Viegas-Aldrovandi, S. M., and Contini, M. 1989, *Astr. Ap.*, submitted.
Ward, M. 1988, paper presented at IAU Symposium 134, *Active Galactic Nuclei*, Santa Cruz, CA, in press.
Ward, M., and Morris, S. 1984, *M.N.R.A.S.*, **207**, 867.
Wilson, A. S., and Ulvestad, J. S. 1982, *Ap. J.*, **263**, 576.
Woods, D. T., Shull, J. M., and Sarazin, C. L. 1981, *Ap. J.*, **249**, 399; (errata: 1982, *Ap. J.*, **257**, 918).
Wu, C-C., and Weedman, D. W. 1978, *Ap. J.*, **223**, 798.

G. J. Ferland and K. T. Korista: Department of Astronomy, Ohio State University, 174 West 18th Avenue, Columbus, OH 43210